Research Article

Received: 2 October 2018 Revised: 23 January 2019 Accepted article published: 22 February 2019 Published online in Wiley Online Library:

(wileyonlinelibrary.com) DOI 10.1002/jsfa.9656

Green synthesis of silver nanoparticles using tomato leaf extract and their entrapment in chitosan nanoparticles to control bacterial wilt

Thaís R Santiago,[a,b] Cínthia C Bonatto,[a,c,d] Maurício Rossato,[c,e] Cláudio A P Lopes,[c] Carlos A Lopes,[e] Eduardo S G Mizubuti[b] and Luciano P Silva[a,c*]

Abstract

BACKGROUND: Silver nanoparticles (AgNPs), particularly those entrapped in polymeric nanosystems, have arisen as options for managing plant bacterial diseases. Among the biopolymers useful for the entrapment of AgNPs, chitosan is promising because of its low cost, good biocompatibility, antimicrobial properties and biodegradability. The present study aimed: (i) to greenly-synthesize AgNPs using different concentrations of aqueous extract of tomato leaves followed by entrapment of AgNPs with chitosan (CH-AgNPs); (ii) to characterize the optical, structural and biological properties of the nanosystems produced; (iii) to evaluate the antimicrobial activities of AgNPs and nanomaterials; and (iv) to assess the effectiveness of AgNPs and nanomaterials for controlling tomato bacterial wilt caused by *Ralstonia solanacearum*.

RESULTS: Spherical and oval AgNPs had incipient colloidal instability, although the concentration of the tomato leaf extract influenced both size (< 87 nm) and the polydispersity index. Nanomaterials (< 271 nm in size) were characterized by a highly stable matrix of chitosan containing polydisperse AgNPs. Free AgNPs and CH-AgNPs were stable for up to 30 days, with no significant alteration in physicochemical parameters. The AgNPs and nanomaterials had antibacterial activity and decreased bacterial growth at micromolar concentrations after 48 h. Morphological changes in *R. solanacearum* cells were observed after treatment with CH-AgNPs. The application of CH-AgNPs at 256 μmol L^{-1} reduced the incidence of bacterial wilt in a partially resistant tomato genotype but not in the susceptible line.

CONCLUSION: Greenly-synthesized chitosan-derived nanomaterials containing AgNPs produced with leaf extracts from their own species appear to comprise a promising and sustainable alternative in an integrated management approach aiming to reduce the yield losses caused by bacterial wilt.

Keywords: antibacterial; biosynthesis; bacterial wilt; eco-friendly; green nanotechnology

INTRODUCTION

Over 200 bacteria species can cause diseases in plants.[1] Control practices for the management of bacterial diseases are very limited and there is an urgent need to develop truly effective solutions to this problem. Traditionally, the most common strategies to control bacterial diseases are crop resistance obtained either by conventional breeding programs or genetically-modified varieties, crop rotation, water management, planting clean materials (seeds or plant parts) and chemical sprays using copper compounds.[2] However, the threat posed by antibiotic resistance led to the ban of this class of antimicrobial compounds for managing bacterial diseases in plants, with the other approaches being only partially effective.[2] Thus, additional plant disease control methods that are effective and environmental-friendly will likely play a major role over the coming years.

The antimicrobial properties of silver nanoparticles (AgNPs) have been examined in different areas because of their strong and wide range of action.[3] These nanostructures have variable shapes and sizes, depending on the synthesis process. Several studies successfully reported the biosynthesis of AgNPs using plant materials as reducing agents, such as *Anacardium othonianum*,[4] *Aloe vera*,[5] *Emblica officinalis*,[6] *Artemisia absinthium*,[7] *Pelargonium* sp.[8] and *Ilex paraguariensis*[9] as a result of the eco-friendly and simple processes required for their synthesis.

* *Correspondence to: L P Silva, Laboratório de Nanobiotecnologia (LNANO), Embrapa Recursos Genéticos e Biotecnologia, PBI, Brasília, 70770-917, DF, Brazil. E-mail: luciano.paulino@embrapa.br, lucianopaulinosilva@gmail.com*

a *Laboratório de Nanobiotecnologia (LNANO), Embrapa Recursos Genéticos e Biotecnologia, Brasília, Brazil*

b *Departamento de Fitopatologia, Universidade Federal de Viçosa, Viçosa, Brazil*

c *Instituto de Ciências Biológicas, Universidade de Brasília, Brasília, Brazil*

d *Pesquisa Aplicada, TecSinapse, São Paulo, Brazil*

e *Laboratório de Fitopatologia, Embrapa Hortaliças, Brasília, Brazil*

The activity of AgNPs has been cosidered and several mechanisms of action have been proposed, such as inhibition of respiration, reduction in enzyme and protein functions, and interaction with phosphorus in DNA, which impairs cell replication.[10] Apparently, Ag^+ ions and AgNPs have similar actions. However, there is an enhanced antibacterial activity for AgNPs mainly as a result of an increase in the amount of Ag^+ locally released upon association with bacterial cells. Additionally, the routes by which nanomaterials are synthesized affect their effectiveness, decrease the toxicity by directing the metal to a specific target, and increase the antimicrobial activity.[11]

Chitosan is a biopolymer that is frequently used to stabilize metal nanoparticles, including AgNPs, as a result of its adsorption properties, biodegradability and non-toxic effects.[12–14] When combined with silver-based materials, chitosan nanoparticles have synergistic effects that contribute toward enhancing antimicrobial properties.[15] Moreover, their antimicrobial activities and the capability of inducing immunity in plants contribute to the increasing interest in the use of this biopolymer.[12]

The major bacterial genera that infect plants are *Pseudomonas*, *Agrobacterium*, *Xanthomonas*, *Erwinia*, *Xylella*, *Pectobacterium*, *Dickeya* and *Ralstonia*.[16,17] Plant pathogenic species of *Ralstonia* cause bacterial wilt, which is a devastating disease that still lacks effective control. Among them, *R. solanacearum* (Smith) is one the most well-known plant pathogenic species.[18] This pathogen has an extensive host range, spanning beyond 50 botanical families and showing a worldwide distribution.[19,20] Despite the large number of host species, bacterial wilt is more intensively studied in banana (*Musa* sp.) (in which it is also known as Moko disease) and in solanaceous plants, particularly on potato (*Solanum tuberosum* L.) and tomato (*Solanum lycopersicum* L.).[21] The pathogen infects tomato plants via wounds and secondary roots, then invades the xylem, where the bacterial population can rapidly increase, causing degradation of the occluded vessels, wilt and plant death.[22] Currently, no chemical compound is used to control bacterial wilt. Nevertheless, the losses experienced in many crops as a result of bacterial wilt, particularly in the tropics, where it affects important staple crops in poor countries, require the assessment of as many new products as possible.

Recent studies using different nanomaterials to control *R. solanacearum* have shown promising results. Imada *et al.*[23] demonstrated a reduced incidence of root infection of tomato seedlings drenched with MgO nanoparticles prior to inoculation with *R. solanacearum*. This treatment probably induced systemic resistance in tomato. In another study, single-walled carbon nanotubes and graphene oxide damaged the cell membrane and led to the release of cytoplasmic material of a copper-resistant strain of *R. solanacearum*, resulting in strong antibacterial activity.[24] Chitosan polymer functionalized with cinnamic acid also controlled the mulberry bacterial wilt pathogen.[25] The use of AgNPs stabilized with polysorbate 80 showed increased bacterial activity against *R. solanacearum* compared to AgNPs alone. Severe damage to the bacterial cell membrane, destruction of cellular proteins and a reduction of the incidence of wilt were observed in tobacco.[26] Similarly, phytofabrication of AgNPs using an aqueous extract of *Helianthus tuberosus*,[27] mangrove associate *Hibiscus tiliaceus* leaf extract[28] and red algae *Hypnea musciformis*[29] were shown to be excellent antibacterial candidates against *R. solanacearum in vitro*. However, to date, all of the studies using AgNPs to control *R. solanacearum* were conducted only *in vitro*. Additionally, to our knowledge, no study has assessed the effects of AgNPs synthesized using tomato leaf extracts associated with chitosan against any soil inhabitant plant pathogenic bacteria. Thus, the present study aimed to: (i) synthesize and characterize AgNPs using different concentration of tomato leaf extract and AgNPs associated with chitosan; (ii) evaluate the *in vitro* antimicrobial activities of the synthesized AgNPs and chitosan-based silver nanomaterials; and (iii) assess the efficacy of AgNPs and chitosan-based silver nanomaterials with respect to controlling bacterial wilt in tomato plants.

MATERIALS AND METHODS

Plant extract

Tomato leaves were collected from 45-day-old asymptomatic tomato plants of cultivar Duradouro grown in a greenhouse in Gama, Federal District, Brazil. The leaves were immersed in a solution of Extran® detergent (Merck Millipore, Burlington, MA, USA) diluted 1000× in distilled water and rinsed with deionized water. After being dried at room temperature, the leaves were weighed, ground with liquid nitrogen and stored in polypropylene tubes at −20 °C until use. One gram of leaves was boiled in 10 mL of deionized water using a heater plate for 2 min. The material was filtered through Qualy No. 7 (14 μm pore) filter paper (Qualy Comercial Eireli, Passos, MG, Brazil). The final volume was adjusted to 10 mL. The light green aqueous extract filtrate was used to produce the AgNPs.

Synthesis and characterization of silver nanoparticles

Three different concentrations of aqueous extract filtrate (derived from 5, 10 and 20 mg of leaf mL^{-1}) were evaluated as phytochemical precursors for the formation of AgNPs. Silver nitrate ($AgNO_3$) (Sigma-Aldrich, St Louis, MO, USA) was used as the precursor metal salt in aqueous solution to a final concentration of 1 mmol L^{-1} for the synthesis of AgNPs. Each one of the synthesis reactions was evaluated with their respective aqueous extract and $AgNO_3$ used as negative controls, and absorbance readings occurred after 0, 1, 2, 4, 8, 12, 16, 20 and 24 h of incubation at 50 °C. AgNPs produced by using tomato leaf extract at concentrations equivalent to 5, 10 and 20 mg of leaf mL^{-1} were named as 5AgNPs, 10AgNPs and 20AgNPs, respectively. Visible absorbance curves at 450 nm of the reactions of 5AgNPs, 10AgNPs and 20AgNPs were obtained over 24 h of monitoring. In addition, the synthesized AgNPs were evaluated throughout the wavelength range of 350–550 nm using plastic cuvettes of 1 cm light path in a ultraviolet (UV)-visible spectrophotometer Q898U (Quimis, Diadema, Brazil) after 24 h to determine the maximum absorbance peaks.

Measurements of hydrodynamic diameters (HD), Zeta potentials and polydispersity indexes (PdI) were performed using the Zeta-Sizer Nano ZS (Malvern Instruments, Malvern, UK) instrument with a He–Ne laser (4 mW) operated at 633 nm for the dynamic light scattering (DLS) technique for the determination of the HD and PdI, as well as electrophoretic mobility, for the assessment of the Zeta potential. For each analysis, samples were diluted with deionized water at a ratio of 1:20. The samples were analyzed in triplicate, with the number of steps in automatic mode, and the scattering angle was set to 173° at 25 °C. Data were analyzed using the Zeta-Sizer software (Malvern Instruments). The processes of synthesis and measurements of HD, Zeta potential and PdI of AgNPs were repeated three times to assess reproducibility.

Synthesis of chitosan nanoparticles

AgNPs immersed in a polymeric matrix of chitosan were produced using the ionic gelation method with the addition of sodium

tripolyphosphate (TPP) as a cross-linking agent. Polymeric solution was prepared with 2 mg mL^{-1} of low molecular weight chitosan (Sigma-Aldrich) dissolved in 0.3 mol L^{-1} acetic acid solution for 1 h with magnetic stirring followed by filtration through a cellulose acetate membrane with pores of 0.22 µm. The solution was mixed with AgNPs (equivalent to 100 µg mL^{-1} $AgNO_3$) synthesized using 5 or 10 mg of leaves mL^{-1} and previously named 5AgNPs and 10AgNPs, respectively. Two milliliters of TPP aqueous solution (8 mg mL^{-1}) was added dropwise over 1 min. The polymeric nanomaterials containing AgNPs were named 5CH-AgNPs (chitosan, TPP and AgNPs synthesized using 5 mg of ground leaves mL^{-1}), 10CH-AgNPs (chitosan, TPP and AgNPs synthesized with 10 mg of ground leaves mL^{-1}) and their respective controls (chitosan, TPP and extract of 5 or 10 mg of ground tomato leaves without $AgNO_3$), named 5CH and 10CH, respectively. The stability of the AgNPs and polymeric nanomaterials was assessed twice at 30-day-intervals using the ZetaSizer Nano ZS (Malvern Instruments). The process of synthesis of nanosystems was repeated three times to assess reproducibility. Statistical analyses were conducted using one-way analysis of variance (ANOVA) test followed by the least significant difference mean comparison test (at $P = 0.05$) using the R software.[30]

Transmission electron microscopy and atomic force microscopy

Transmission electron microscopy (TEM) and atomic force microscopy (AFM) were used to characterize the shape, distribution and size of: (i) AgNPs and chitosan nanomaterials and (ii) the morphology of bacterial cells before and after treatment with the nanomaterials. AgNPs and chitosan nanomaterials were diluted in water (1:100) and deposited onto Formvar-coated copper grids before the analysis and kept in a protected cabinet overnight to dry. TEM images were obtained using a JEM-1011 transmission electron microscope (Jeol, Tokyo, Japan) with a work voltage of 100 kV. The AFM images were acquired in dynamic mode, at 512 × 512 lines resolution using a Shimadzu SPM-9600 (Shimadzu Corp., Kyoto, Japan) equipped with a scanner with maximum x and y dimensions of 125 µm. The images were processed to correct the scan plane with the offline software provided with the instrument. Bacterial cells treated or not with 64 and 128 µmol L^{-1} of 10CH-AgNPs for 48 h were examined after fixation in methanol and deposited onto a glass circular coverslip. The analyses were performed in contact mode, with areas of 12.5 × 12.5 μm^2 at 512 × 512 lines resolution. The images were processed to correct the scan plane and the average roughness of bacterial cells were performed from 100 measurements in areas of 40 × 40 nm^2 using the offline software.

In situ Fourier-transform infrared spectroscopy studies

Fourier-transform infrared spectroscopy (FTIR) analyses allowed the identification of probable functional groups of compounds potentially involved in the process of reduction and stabilization of AgNPs and chitosan nanomaterials. The spectra were obtained using a Vertex 70 (Bruker Corporation, Billerica, MA, USA) spectrometer in the attenuated total reflectance configuration with the liquid samples. Two microliters of each sample were deposited onto a diamond crystal and the analyses were carried out in the region between 4000 to 350 cm^{-1}, with resolution of 4 cm^{-1} and 32 scans. Data were acquired and processed using OPUS, version 7.2 (Bruker Corporation).

In vitro study

To determine the minimum inhibitory concentration of the AgNPs, RS489 isolate of *R. solanacearum*, characterized as phylotype II, biovar 1 (Culture Collection of Embrapa Hortaliças, Brasília, Brazil) was cultivated in liquid CPG medium without tetrazolium[31] for 48 h at 28 °C. Cell suspensions were adjusted to obtain an optical density at a wavelength of 600 nm (OD_{600}) = 0.100 with a spectrometer Q798U (Quimis), which corresponds to approximately 10^8 ufc mL^{-1}. Twenty microliters of bacterial cells were added to 180 µL of CPG medium with AgNPs/CH-AgNPs and dispensed in a well of a microplate. The pathogen was exposed to different AgNPs (5AgNPs and 10AgNPs) and chitosan nanomaterials (5CH-AgNPs and 10CH-AgNPs), at different concentrations: 4, 16, 32, 64, 128 and 256 µmol L^{-1}. Distilled sterilized water, chitosan solution and Ag^+ were used as controls. The minimum inhibitory concentration was assessed in three replicates (one well of the plate was considered as a replicate). The microplates were sealed with Parafilm and kept at 28 °C for 24 and 48 h. The optical density (OD_{600} nm) was measured after 24 and 48 h with the microplate reader ELX 808 IU (Biotek Instruments Inc., Winooski, VT, USA). The rate of growth was determined by subtracting OD_{600} data of the time 0 h from the data at 24- and 48-h intervals. ANOVA assumptions (normality and homoscedasticity of the errors) were checked and the results were expressed as the mean ± SEM by AgNPs or CH-AgNPs/concentration/day. Statistical analyses were performed with the R software.[30] The fitted logistic curves were constructed to analyze the concentration required to inhibit 50% and 90% of bacterial growth (IC_{50} and IC_{90}, respectively.

In vivo study

Two contrasting tomato cultivars, Ellen, partially resistant, and, L390, susceptible to bacterial wilt, were sown in 128-cell polyethylene trays, containing Plantmax (Terralift, Market Deeping, UK) substrate. Plants were grown for 40 days in a greenhouse (28 ± 3 °C), and then treated with 1 mL of AgNPs (5AgNPs and 10AgNPs) and chitosan nanomaterials (5CH-AgNPs, 5CH, 10CH-AgNPs, 10CH) at 128 or 256 µmol L^{-1} (equivalent concentration to $AgNO_3$) and the extract of tomato leaves (5E and 10E). Treatments were applied by pipetting nanoparticles and nanomaterials directly to the surface of the substrate, near the roots. Plants treated with water were used as controls. After 2 days, treated seedlings were sprayed with *R. solanacearum* (OD_{600} = 0.100) with one spray application of approximately 1 mL of the suspension in each side of the substrate of the seedling. After inoculation, plants were removed of the polyethylene trays and transplanted to pots with sterile soil mixture, one plant by 0.5 L pot. Each treatment was applied to 10 experimental units (one experimental unit = one plant pot^{-1}). Three replicates of each treatment were assessed at different times (three blocks of 10 plants each). Wilt incidence was evaluated every 2 days, from day 2 up to day 15 after pathogen inoculation. Incidence was calculated as the ratio between the number of wilted plants divided by the total number of plants at the beginning of the evaluations multiplied by 100 to express the results in percentage. A plant with any symptom of wilt was considered as an infected. Disease progress was assessed by plotting incidence data over time and the area under the disease progress curve (AUDPC) was calculated for each treatment. AUDPC values were subjected to ANOVA, and protected Fisher's least significant difference test at $\alpha = 0.05$ was used to compare treatment means.

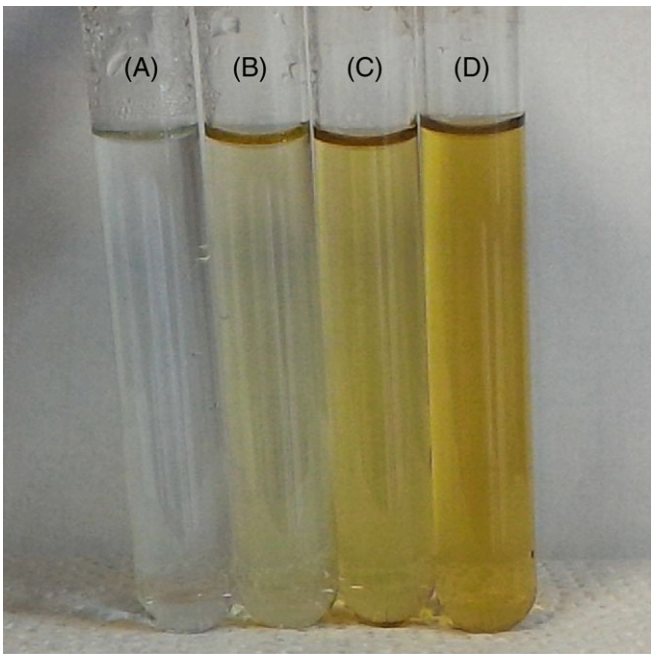

Figure 1. Reaction tubes containing an aqueous solution of Ag^+ (A) and suspensions of AgNPs synthesized using 5 (B), 10 (C) and 20 (D) mg mL^{-1} of tomato extract over 24 h.

RESULTS

Optical properties, structure and Zeta potential of silver nanoparticles

After 24 h of reaction between $AgNO_3$ and the aqueous extract of tomato leaves, there was a change in color, which is considered as indicative of the formation of AgNPs. In all reaction tubes, a yellow color colloidal suspension was observed, except in those reactions with only extract of tomato leaves (5E and 10E, data not shown) or Ag alone (Fig. 1). There was an increase in the absorbance around 450 nm (Fig. 2A). Moreover, the absorbance values of 5AgNPs, 10AgNPs, 20AgNPs and free Ag reactions were also measured in the visible region of the electromagnetic spectrum (350–550 nm) using UV–visible spectroscopy. Except for the AgNPs synthesized using 20 mg of extract mL^{-1}, the other treatments resulted in an increase in UV-visible spectra above 400 nm. A peak with absorbance between 430–440 nm was observed in 5AgNPs, indicating the formation of AgNPs (Fig. 2A). An increase of absorbance was observed with the increase of the extract concentration (Fig. 2B). No peak was detected in free Ag, thus there was no evidence of any nanostructure formation and hence no evidence of a surface plasmon resonance (SPR) effect (Fig. 2B).

Different physical characteristics were observed using DLS, electrophoretic mobility (Zeta potential) and TEM analyses. DLS allowed determination of the HD of suspended particles by light scattering and the distribution of population sizes of the particles analyzed by determining the PdI, and electrophoretic mobility allowed determination of the particles surface Zeta potential. The HD (*Z*-average) for the 5AgNPs and 10AgNPs suspensions was 51.9 ± 11.6 nm with a bimodal distribution and 86.3 ± 1.5 nm with an unimodal distribution, respectively (Fig. 3F and Table 1).

According to Murdock *et al.*,[32] the PdI value of around 0.500 observed for 5AgNPs indicated a polydisperse distribution. Otherwise, when 10 mg mL^{-1} of extract of tomato leaves was used in the reaction medium (10AgNPs), monodisperse nanoparticles were observed (PdI = 0.22 ± 0.01). Indeed, the present study showed that the amount of extract of tomato leaves influenced the size and PdI of the AgNPs (Table 1). The Zeta potentials of both AgNPs synthesized were negative: -13.7 ± 1.6 and -20.1 ± 1.6 mV for 5AgNPs and 10AgNPs, respectively. Based on these values, the AgNPs were classified as having incipient instability (Table 1).

The higher concentration of tomato leaf extract evaluated regarding the potential to synthesize AgNPs (20 mg mL^{-1}) resulted in sub-micrometric particles with an HD of 551.2 ± 17.7 nm, 0.732 ± 0.2 of PdI and 14.0 ± 0.8 mV of Zeta potential (data not shown). Indeed, the antibacterial activity of 20AgNPs was not investigated as a result of the high precipitation after synthesis, as well as the high HD size of these particles, and thus no evidence of AgNPs formation in the SPR test.

To attempt to enhance the stability, penetration and effectiveness, AgNPs synthesized with 5 and 10 mg mL^{-1} were coated with chitosan of low molecular mass and then named 5CH-AgNPs and 10CH-AgNPs, respectively. The average HD for the 5CH-AgNPs and 10CH-AgNPs nanomaterials was 249.5 ± 7.8 and 270.9 ± 5.8 nm, respectively, and the formation of a matrix containing AgNPs was observed (Fig. 4A). Recently synthesized 5CH-AgNPs and 10CH-AgNPs were characterized with PdI > 0.400 and a positive Zeta potential around 50 mV, indicating polydisperse and highly stable nanomaterials (Fig. 4B,C).

Additional characterization of size, shape and agglomeration of AgNPs and chitosan nanomaterials was accomplished using TEM (Fig. 3A–D). There was high concentration of non-agglomerated spherical and anisotropic AgNPs, which occurred in varied sizes and with irregular edges coated by a capping agent (Fig. 3A,B). The same pattern was observed in the nanomaterials 5CH-AgNPs and 10CH-AgNPs (Fig. 3C,D). Chitosan molecules were not observed using this technique. The size (dry diameter) of AgNPs and nanomaterials averaged 35 and 50 nm, respectively. There was difference in size comparing different concentrations of leaf extracts among AgNPs and nanomaterials based on measurements obtained from TEM; however, there was no difference in size for AgNPs with or without chitosan in their composition ($P > 0.05$) (Fig. 3E).

Stability and reproducibility of synthesized AgNPs and chitosan nanomaterials

The synthesized AgNPs and chitosan nanomaterials were stored at 10 °C for 60 days. The kinetic stabilities were evaluated based on size, PdI and Zeta potential as assessed at 0, 30 and 60 days after synthesis. The nanoparticles (5AgNPs and 10AgNPs) and nanomaterials (5CH-AgNPs, 5CH, 10CH-AgNPs and 10CH) were stable for up to 30 days, without any significant changes in size, PdI and Zeta potential. After 60 days of synthesis, the PdI value of 5AgNPs and the size of 10AgNPs changed ($P < 0.05$) (Fig. 4A–C). Additionally, the Zeta potential values also varied ($P < 0.05$) (Fig. 4C). For the nanomaterials based on chitosan, the main alteration was registered for the size of the particles 5CH, 10CH and 10CH-AgNPs ($P < 0.05$) (Fig. 4A). There was also a change in PdI value for the 5CH-AgNPs. No significant differences were observed among nanomaterials in Zeta potential values (Fig. 4C). No differences were observed among the results from the three syntheses of nanoparticles (5AgNPs and 10AgNPs).

FTIR

FTIR measurements were carried out to identify the possible functional groups present in biomolecules from *S. lycopersicum* leaf extract and their role in the synthesis of AgNPs, as well as the role of

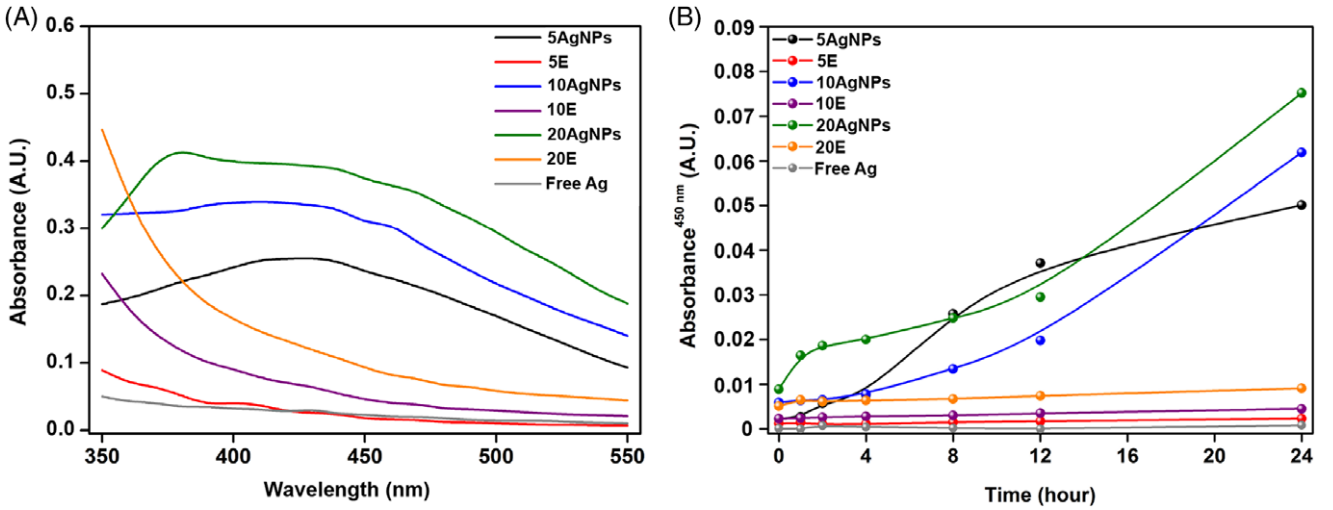

Figure 2. Visible absorbance curves of 5AgNPs, 10AgNPs and 20AgNPs (and controls) in wavelengths ranging from 350 to 550 nm after 24 h (A) and kinetics of formation of AgNPs produced with 5, 10 and 20 mg mL^{-1} of tomato leaf extract named 5AgNPs, 10AgNPs and 20AgNPs (and controls), respectively (B).

molecules as coating agents. The spectra of the extract of *S. lycopersicum* showed absorption bands at 2922, 2852, 2360, 2674, 1602, 1431, 1201, 1136 and 1045 cm^{-1} (Fig. 5). The band at 2922 cm^{-1} is an indication of aliphatic stretching. The band at 2360 cm^{-1} can be assigned to the stretching vibration of olefinic compounds. The absorption in the region of 1602 cm^{-1} suggests the axial vibration of C=C double bonds in aromatic groups. The band at 1431 cm^{-1} indicates carboxylate groups. The peak at 1201 cm^{-1} refers to the C-O and the band near 1045 cm^{-1} is an indication of C-O-C stretching. The AgNPs spectrum presented the same bands as tomato leaf extract but with suppression of the bands at 2922 and 2852 of cm^{-1}, and the occurrence of a band at 1350 cm^{-1}, which possibly related to the NO stretching mode of the nitric functional groups. Upon the addition to chitosan, the absorption bands at 1599 and 2365 cm^{-1} are related to chitosan shifts.[33–35] The band at 1413 cm^{-1} is characterized by the stretching vibration of the amino group in chitosan, and the peaks in the range 1070–1028 cm^{-1} represent the saccharide structure of chitosan.

AgNP biological properties in vitro and in vivo

The effects of six concentrations of AgNPs and chitosan nanomaterials against *R. solanacearum* were tested *in vitro*. The nanomaterials 5AgNPs, 10AgNPs, 5CH-AgNPs, 5CH, 10CH-AgNPs and 10CH completely inhibited the growth of *R. solanacearum* at 64, 128 and 256 µmol L^{-1} when tested at 24 and 48 h of incubation. Tests based on incubation with equivalent concentrations of tomato leaf extracts did not differ from the control plant treated with water.

A sigmoidal logistic curve was fitted to the bacterial wilt progress upon plant inoculation. The r^2 values were higher than 0.90 and the SEs values were low, indicating a proper model fit to the data. After 24 h, based on the logistic curves, IC_{50} and IC_{90} values were calculated and the lowest values were found for free Ag^+, 5AgNPs and 10AgNPs, varying from 9.1 (5.7–12.5) to 18.0 (10.6–25.3) µmol L^{-1} for IC_{50}, and 30.2 (18.9–41.4) to 58.9 (41.5–77.3) µmol L^{-1} for IC_{90} (Table 2). The IC_{50} and IC_{90} values of nanomaterials had very similar results compared to chitosan. However, after 48 h the lowest values for IC_{50} and IC_{90} indicated a better activity of nanomaterials (5CH-AgNPs and 10CH-AgNPs) and chitosan (5CH and 10CH) compared to 5AgNPs and Ag^+. These results suggest that nanomaterials inhibit bacteria more effectively after 24 h upon contact. In addition, the 10AgNPs was the most effective formulation for inhibiting the growth of *R. solanacearum in vitro*.

Both 5CH-AgNPs and 10CH-AgNPs resulted in the smallest values of AUDPC when investigating the chitosan nanomaterials 5CH-AgNPs and 10CH-AgNPs with respect to controlling bacterial wilt in tomato plants (Fig. 6). Moreover, 5CH-AgNPs and 10CH-AgNPs were more effective compared to 5AgNPs, 10AgNPs, 5CH and 10CH at concentrations of 128 and 256 µmol L^{-1} ($P < 0.001$) in Ellen cultivar. Apparently, the amount of extract does not change the *in vivo* activity against *R. solanacearum* as observed for nanomaterials produced with 5 and 10 mg mL^{-1} of tomato leaf extract. All other treatments and chitosan nanomaterials applied at the concentration equivalent to 128 µmol L^{-1} did not differ from the control and no phytotoxicity was observed. Randomly selected wilting plants tested positive for the ooze test in water, thus indicating that *R. solanacearum* was the sole agent responsible for this symptom.

Concentration-dependent effect of silver nanoparticles in bacteria and colony morphology

The effect of concentration of 10CH-AgNPs in *R. solanacearum* was assessed after 48 h (Fig. 7). The roughness of the bacterial cell wall increased with nanomaterial concentration. The average nanoroughness value for *R. solanacearum* cell wall was 400 nm at 64 µmol L^{-1} (Fig. 7B), whereas it was near 500 nm at 128 µmol L^{-1}, and the cell length increased (Fig. 7C). At 64 and 128 µmol L^{-1}, it was possible to observe protuberances on cell wall, with a higher intensity at a higher concentration of AgNPs.

DISCUSSION

The antibacterial activity of green-synthesized AgNPs is reported, both *in vitro* and *in vivo*, as an alternative for managing bacterial wilt caused by *R. solanacearum*. Different studies have shown that plant extracts and microorganisms can be used to reduce silver ion to form silver nanoparticles with peculiar physicochemical and biological activities.[8,36] The biosynthesis of AgNPs mediated by different concentrations of tomato leaf extract was efficient with respect to producing biologically active AgNPs against *R. solanacearum*. Tomato fruit extracts have been used previously to

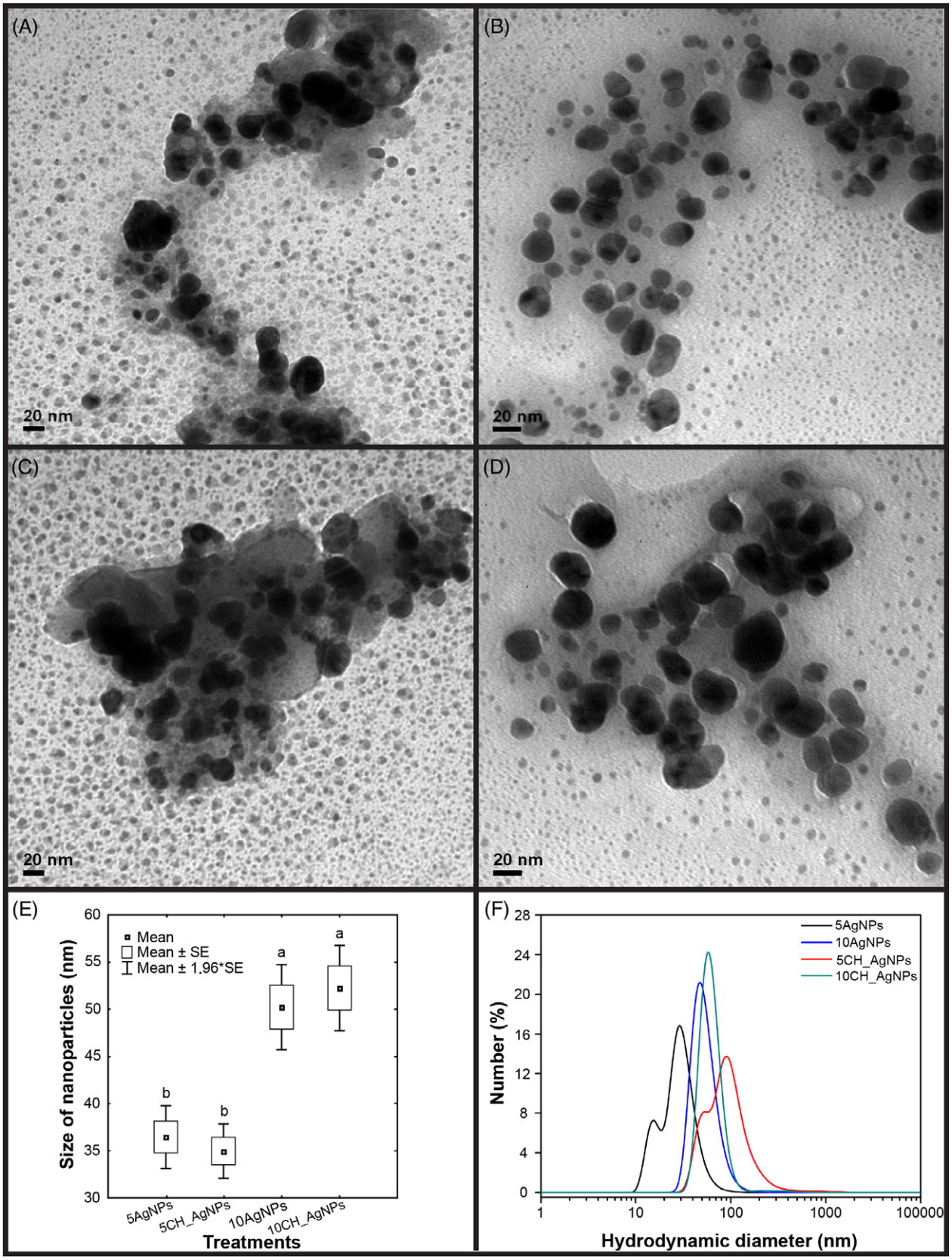

Figure 3. Transmission electron micrographs of AgNPs synthesized using 5 mg mL^{-1} tomato leaf extract (5AgNPs) (A) or 10 mg mL^{-1} tomato leaf extract (10AgNPs) (B), nanomaterial derived from 5AgNPs associated with chitosan (5CH-AgNPs) (C), nanomaterial derived from 10AgNPs associated with chitosan (10CH-AgNPs) (D), dry diameter assessed by TEM of AgNPs and chitosan-based nanomaterials (E) and hydrodynamic diameter dispersion of nanoparticles and nanomaterials (F). Scale bars = 20 nm.

Table 1. Nanoparticles size (nm), polydispersity index (PdI) and Zeta potential of two types of AgNPs produced with different concentrations of tomato leaf extract (5 and 10 mg mL^{-1}) repeated three times

	First synthesis			Second synthesis			Third synthesis		
Nanoparticles	Size (nm)	PdI	Zeta (mV)	Size (nm)	PdI	Zeta (mV)	Size (nm)	PdI	Zeta (mV)
5AgNPs	51.9 ± 11.6	0.501 ± 0.06	−13.7 ± 1.6	53.8 ± 7.0	0.551 ± 0.02	−12.9 ± 0.3	56.4 ± 4.8	0.510 ± 0.01	−15.4 ± 1.4
10AgNPs	86.3 ± 1.5	0.222 ± 0.01	−20.1 ± 1.6	92.6 ± 6.8	0.292 ± 0.01	−14.8 ± 2.1	84.3 ± 3.6	0.273 ± 0.01	−13.1 ± 0.8
Ag^+	119.7 ± 2.5	0.113 ± 0.01	−20.1 ± 0.7						

reduce additional toxic products generated during the synthesis of nanoparticles.[37] In the present study, we report on the use of tomato leaf extract to reduce silver ions into AgNPs.

Different concentrations of extract from tomato leaves modulated the synthesis of AgNPs. There was a gradual increase of absorbance with the increase in the amount of extract added to the reactions. The increase in absorbance could be correlated with possible differences in size, shape, composition, reduction yield and/or surface chemistry of AgNPs.[38,39] Based on the UV-visible curves indicative of the SPR phenomenon, there were differences in the size and/or shape of AgNPs, as well as the biological activity of AgNPs, synthesized with different concentrations of tomato leaf extract. However, some studies report that the reaction time, temperature and concentration of the plant extract modify the reduction of Ag^+. In the present study, at the highest concentrations (10–20 mg of extract mL^{-1} of tomato leaves), the reduction of silver ions was apparently decreased with a slight absorbance peak below 400 nm, which is different from that observed during the formation of 5AgNPs. The presence and the increase of an unknown substance in the extract could have inhibited the formation of AgNPs. Shahverdi *et al.*[40] found that piperitone, a natural product of Enterobacteriaceae, is involved in preventing the reduction of Ag^+ into AgNPs. The possible presence of this or others inhibitory agents in aqueous tomato extract needs to be investigated further.

Functional groups of molecules such as carbohydrates, flavonoids, phenolic compounds, phenolics acids, proteases and terpenoids have been identified as being responsible for reducing Ag^+ to Ag^0 in the green synthesis of AgNPs.[41–43] FTIR analysis allowed the investigation of possible interactions between silver and biomolecules involved in the biosynthesis of AgNPs, resulting in nanoparticle stabilization.[44,45] In the present study, the FTIR spectra of AgNPs showed the presence of aromatic and carboxylate groups, which are both constituents of phenolic acids. Indeed, a high concentration of phenolic acids was previously detected in leaf extracts of tomato such as gallic, chlorogenic, ferulic and caffeic acids.[46] Recently, Della Pelle *et al.*[47] demonstrated the importance of phenolic compounds in the reduction, dispersion and stability of AgNPs. Others phenolic compounds typically found in tomato leaf extracts are flavonoids, chlorophyll and carotenoids.[46] Flavonoids are reported in different studies as comprising important reduction agents of AgNPs.[39,48] In the presence of chitosan, the absorption signal of AgNPs is suppressed, indicating a possible coating or entrapment by this biopolymer. Indeed, characteristic bands of chitosan were identified from the nanomaterial spectra.

Tomato leaf extract produced small AgNPs that had moderate stability, a high reproducibility of synthesis, a non-toxic effect in tomato plants, and were active against *R. solanacearum*. In comparison with extracts from the plants *Terminalia chebula*, *Mimusops elengi*, *Myristica fragrans*, *Centella asiatica* and *Hemidesmus indicus*, which were already used to produce AgNPs with good antimicrobial activity, the AgNPs synthesized with tomato leaf extract in the present study showed a smaller size (5AgNPs and 10AgNPs had diameters < 100 nm) and a higher colloidal stability as indicated by the Zeta potential (< −20.1 ± 1.6 mV). In general, a hydrodynamic size between 10–500 nm is commonly found in green synthesis approaches.[49–52] AgNPs biosynthesized using tomato leaf extract are likely to be readily taken up by the plants via penetration by natural openings and can potentially translocate inside the plants as already demonstrated.[53,54] To increase stability and facilitate the movement through the plant cuticle, AgNPs were associated with chitosan molecules, comprising amphiphilic compounds previously used in several studies.[12,13] AgNPs-containing chitosan-based nanomaterial increased the colloidal stability with positive charges. The zeta potential values observed in 5CH-AgNPs and 10CH-AgNPs have sufficient mutual repulsion to ensure the stability of the suspension, making them interesting for application in the field.[55] Another option for increasing the stability without using capped or entrapped AgNPs is to optimize the protocol of the synthesis of AgNPs, as well as extract production (fragmentation of leaves, boiling time), variation of temperature (increase of temperature) and reaction time, which could be investigated further.

Reproducible effectiveness and stability in storage are desirable properties of pesticides. One of the major disadvantages of the use an environmentally friendly procedure for reducing silver is that a minimal variation of secondary metabolites in extract composition could not reproduce the characteristic of particles. The synthesized AgNPs of the present study were obtained from tomato leaves collected only once, macerated, and then frozen ad a powder. This procedure had a high reproducibility and AgNPs were stable for up to 30 days with storage at 10 °C. The HD was the major characteristic altered after 60 days. Stability can be affected by storage temperature over time. Jannoo *et al.*[56] reported that AgNPs were stable after 420 days when stored at 5 °C and the highest stability of the AgNPs was achieved when stored at temperatures even lower than 5 °C. The stability of AgNPs synthesized with tomato leaf extract was not assessed when stored at lower temperatures.

The antibacterial activity of AgNPs increased with the size of the nanoparticles after 24 and 48 h. The 10AgNPs had a higher inhibitory effect on the *in vitro* growth of *R. solanacearum* based on IC_{50} and IC_{90} values compared to other treatments. Differences in the efficiency between the treatments 5AgNPs and 10AgNPs to control *R. solanacearum* could be related to the possible greater formation of AgNPs when 10 mg mL^{-1} of plant extract was mixed with $AgNO_3$ compared to 5AgNPs. Both silver states had similarly high antibacterial activity and toxicity up to 24 h. In other studies, using an equimolar silver solution, Ag^+ ions were more toxic to *Pseudomonas aeruginosa*, *Staphylococcus aureus*, *Saccharomyces cerevisiae* and *Chlorella protothecoides* than AgNPs.[57] Usually, cell

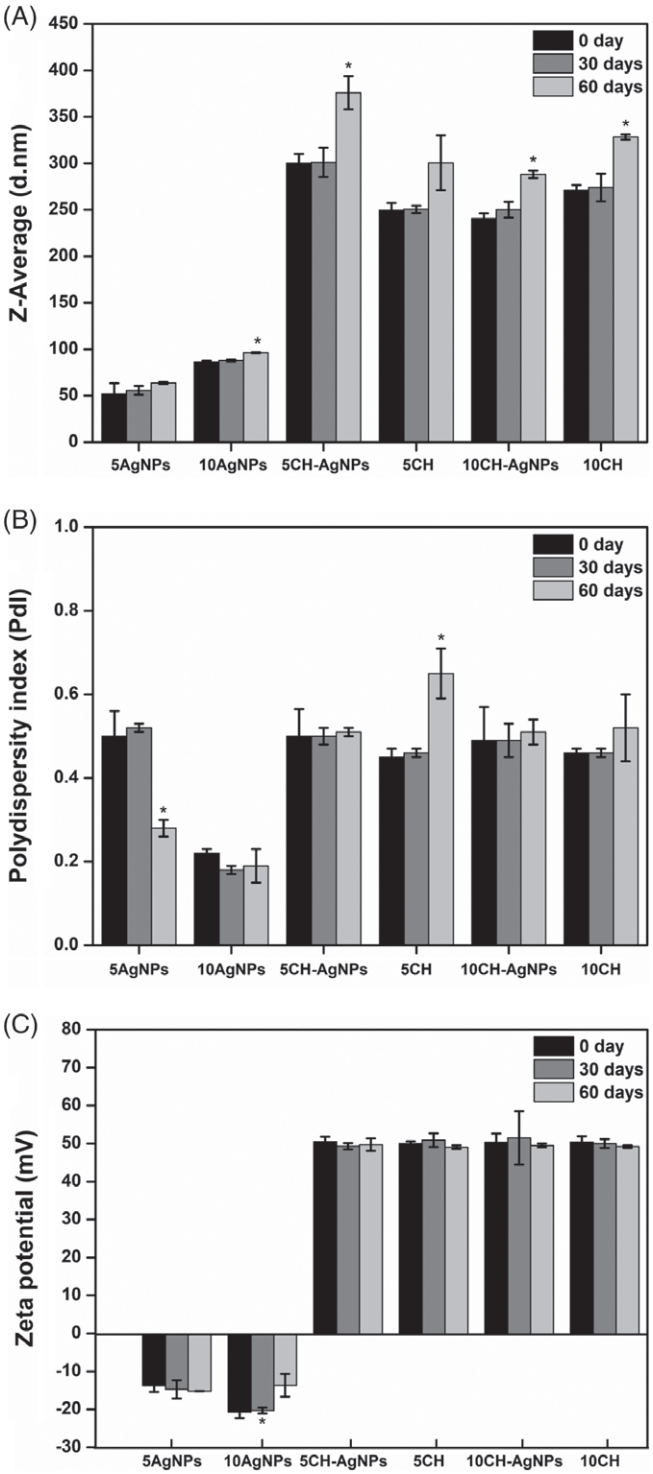

Figure 4. Size (A), polydispersity index (PdI) (B) and Zeta potential (C) of AgNPs and chitosan-based nanomaterials at 0, 30 and 60 days after synthesis.

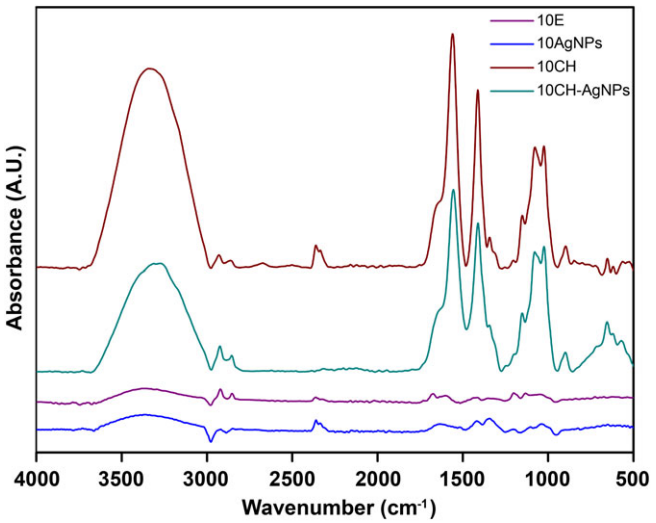

Figure 5. FTIR spectra of tomato leaf extract (10E; purple line), silver nanoparticles (10AgNPs; blue line), chitosan-leaf extract (10CH; red line) and chitosan-AgNPs (10CH-AgNPs; blue line).

mortality is greater when smaller particles are tested because of the greater release of Ag^+ ions as a result of the increased surface area per mass/volume. Indeed, AgNPs of 20 nm were more toxic than particles of 80 nm *in vitro*.[58] This effect was not observed for AgNPs in the present study. Otherwise, chitosan apparently inhibited or prevented the antibacterial activity of AgNPs *in vitro* when the nanomaterials were tested. The interaction between chitosan and AgNPs, avoiding direct contact of the nanoparticles with bacterial cells and a lesser microbicide effect of chitosan compared to AgNPs, could have influenced the lower efficiency as noted in a previous study.[59]

Nanomaterials based on chitosan have interesting properties for use in agriculture, including an increased stability and penetration into the plant; provision of a physical barrier to avoid pathogen penetration; biocompatibility; direct antibiosis against pathogens; promotion of enhancement of beneficial organisms; and stimulation of plant defenses against biotic stresses.[12,13] Chitosan also has intrinsic bacteriostatic and bactericidal effects. *Escherichia coli* bacteria were completely inactivated using chitosan at the concentration of 1% after 2 days of incubation.[60] In the present study, chitosan was effective with respect to inhibiting *in vitro* growth of *R. solanacearum* on the second day, as well as in greenhouse experiments.

The most efficient treatment with respect to preventing the infection of tomato plants was the application of the nanomaterials produced with AgNPs at 256 µmol L^{-1} associated with chitosan in the rhizosphere (pre-infection-treatment). Both 5CH-AgNPs and 10CH-AgNPs were effective when applied as a protective or preventive nanochemical, before plants become infected by *R. solanacearum*. When 5CH-AgNPs and 10CH-AgNPs were applied as post-infection-treatment, the disease intensity did not differ from the control plants that received only water (data not shown). The antimicrobial activities of the nanomaterials are a result of the presence of silver, chitosan or a potential synergistic interaction between them.[15] Similar effects were reported concebring the synergistic activity that contributed to improving biological activity.[61] Additionally, no toxic effect was observed in the tomato plants. Apparently, the absence of toxicity can be related to the biological synthesis route. In a recent study using *S. lycopersicum*, a low toxic effect of biologically-synthesized AgNPs was reported compared to chemically-synthesized AgNPs when introduced in the plant by the petiole.[62]

The less pronounced effects of AgNPs in greenhouse test can be associated with soil interactions and changes in the properties of the particles (i.e. stability and chemistry).[63] Additionally, the success of management of bacterial wilt using AgNPs

Table 2. IC_{50} and IC_{90} values and confidence interval (in parentheses) of AgNPs and AgNPs associated with chitosan (CH-AgNPs) after 24 and 48 h of treatment against Ralstonia solanacearum

	IC_{50} (μmol L^{-1})		IC_{90} (μmol L^{-1})	
Treatments	24 h	48 h	24 h	48 h
10AgNPs	9.1 (5.7–12.5)	18.3 (15.1–21.5)	30.2 (18.9–41.4)	60.8 (50.1–71.5)
10CH-AgNPs	34.2 (26.3–42.0)	49.4 (41.4–57.3)	113.5 (87.4–139.6)	164.1 (137.7–190.3)
10CH	32.1 (24.6–39.4)	44.9 (37.8–52.2)	106.4 (81.7–131.1)	149.4 (125.4–173.3)
5AgNPs	17.7 (12.7–22.7)	77.1 (64.4–89.8)	58.7 (42.1–75.4)	256.1 (213.9–298.2)
5CH-AgNPs	30.8 (23.1–38.5)	49.2 (39.8–58.6)	102.4 (76.8–128.1)	163.4 (132.1–194.8)
5CH	38.1 (29.6–46.6)	62.3 (53.3–71.3)	126.6 (98.2–154.9)	206.8 (177.0–236.7)
Ag^{+}	18.0 (10.6–25.3)	71.6 (59.4–86.9)	58.9 (41.5–77.3)	250.9 (220.2–321.6)

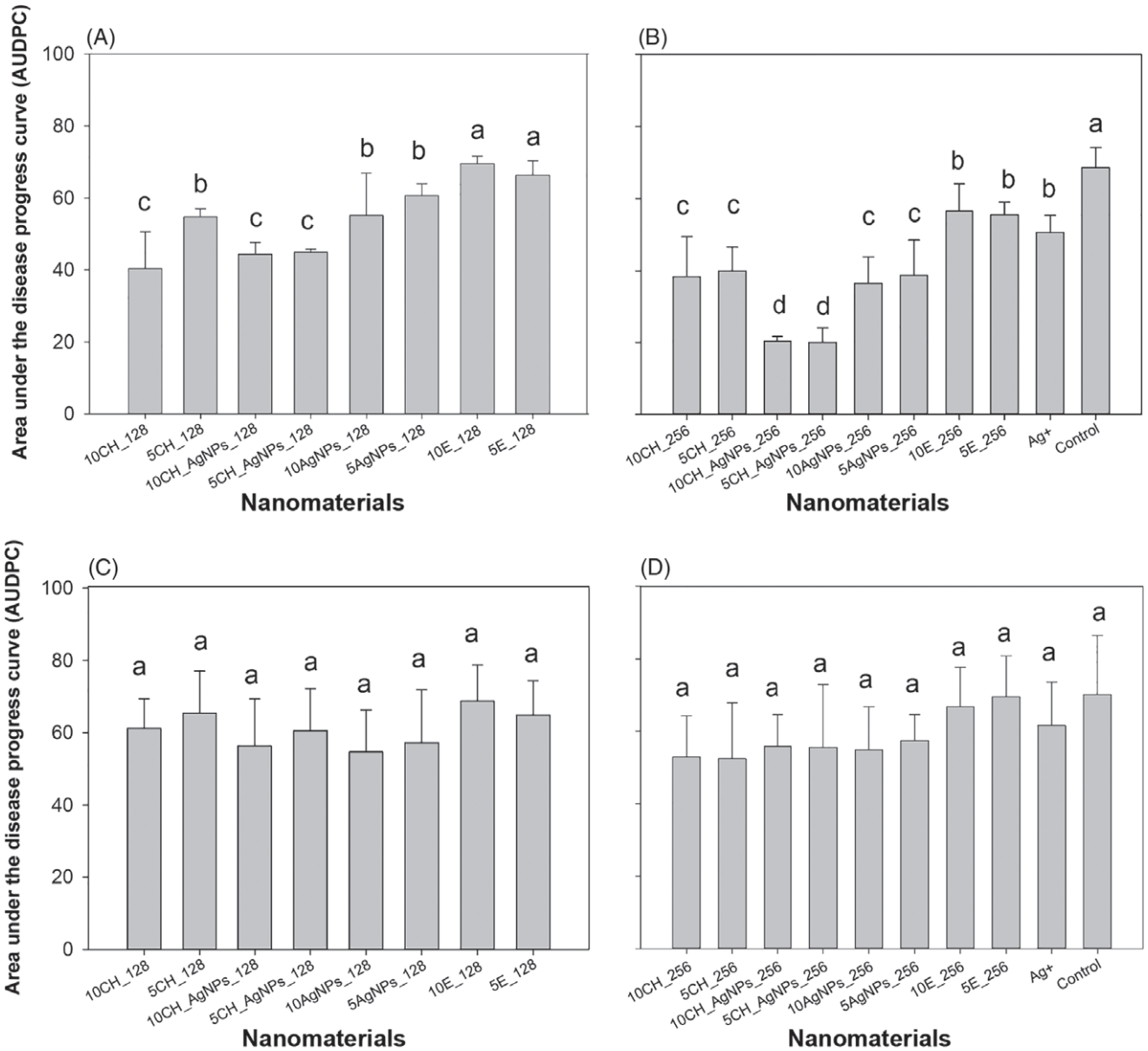

Figure 6. Area under disease progress curve (AUDPC) in the cultivar Ellen (A, B) and cultivar L390 (C, D) by bacterial wilt (*Ralstonia solanacearum*) treated with AgNPs and chitosan-based silver nanomaterials at a concentration of 128 μmol L^{-1} (A, C) and 256 μmol L^{-1} (B, D). Plant wilt was scored every 2 days, up to 15 days after inoculation. Mean AUDPC was calculated using data from three repetitions. Error bars represent the SEM calculated from three repetitions. Treatments are indicated below each bar.

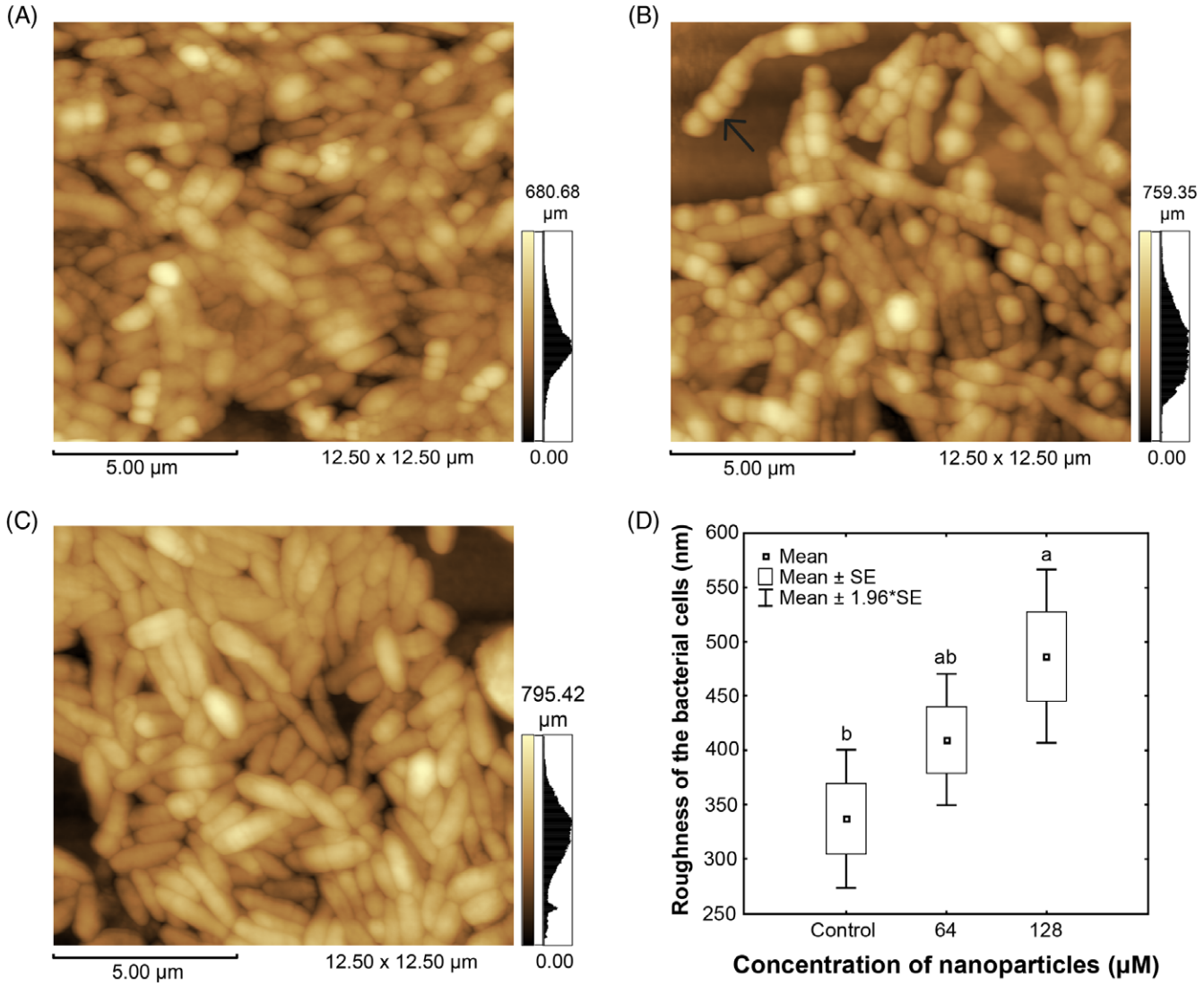

Figure 7. AFM topographies of *R. solanacearum* cells with no pretreatment cells (A), in contact with 10CH-AgNPs at 64 µM (B), in contact with AgNPs at 128 µM for 48 h (C) and AFM roughness results of cell culture incubation (median, minimum–maximum) in the absence/presence of AgNPs at different concentrations (64 and 128 µmol L^{-1}) after 48 h (D). Differences of average roughness values between different AgNPs concentrations were significant ($P < 0.05$, ANOVA). An arrow indicates the observed protuberances.

coated/entrapped with chitosan is cultivar-dependent. Disease control was higher in Ellen than in L390 cultivar. Thus, the results of the present study demonstrate for the first time that the interaction between plant systems and AgNPs induced different defense mechanisms that varied with the cultivar. Chitosan and other nanoparticles (e.g. MgO NPs) are capable of inducing systemic resistance and generating a physical barrier in tomato.[23] The induction of resistance is the major mechanism associated with the control of *R. solanacearum* when plants were pretreated with MgO NP.[23] However, host genotype affects the induction of resistance,[64] which is commonly used to explain differences in disease intensity. Other hypothesis explaining the difference in effects between cultivars is the association of the antagonistic activity of silver/chitosan and also other specific mechanisms intrinsic to each plant cultivar.

The mode of action of Ag^+ ions on microorganisms is well documented. However, the full mechanisms of the effects of AgNPs are still not clear. It is not known whether AgNPs act as a result of their own characteristics or only after releasing the silver ion.[65,66] Silver ions interact with thiol groups present in membrane proteins, leading to their inactivation, thus affecting transport, cell respiration, production of ATP and DNA replication.[67] In addition, AgNPs can affect microbial cells by permeating the cell membrane and interrupting transmembrane electron transfer, promoting oxidation of cell components, and making the cell susceptible to reactive oxygen species.[68] The present study confirmed the bacterial cell damage caused by AgNPs. AFM images of *R. solanacearum* upon contact with AgNPs coated/entrapped with chitosan showed an increase in roughness, size and number of protuberances in the cell wall in a concentration-dependent manner.

CONCLUSIONS

Nanotechnology is a promising area with respect to the development of products for controlling bacterial plant pathogens. AgNPs alone and AgNPs-coated/entrapped with chitosan affected cell integrity *in vitro* and decreased the severity of an important soil pathogen, *R. solanacearum*, both *in vitro* and *in vivo*. In

addition, this green synthesis approach used leaf extract from the same plant species (tomato) that would be targeted for protection against bacterial wilt, aiming to produce AgNPs via a rational and sustainable approach. However, the possible impacts of the residues of AgNPs and nanomaterials in the environment still require more in-depth study, as does an understanding of their dynamics inside the plants, such as translocation of particles and the effects of these nanomaterials against potentially beneficial bacteria. The 5CH-AgNPs and 10CH-AgNPs nanoformulations use a low amount of silver and are inexpensive and eco-friendly. These nanomaterials have the potential for use in an integrated management program; for example, for treating tomato seedlings before they are planted in field.

ACKNOWLEDGEMENTS

This research was supported by the Brazilian agencies Coordenação de Aperfeiçoamento de Pessoal de Nível Superior (CAPES no. 23038.019088/2009-58), Conselho Nacional de Desenvolvimento Científico e Tecnológico (CNPq no. 408857/2016-1, 306413/2014-0, 563802/2010-3 and 470227/2013), Empresa Brasileira de Pesquisa Agropecuária (Embrapa no. 03.17.00.069.00.00, 01.14.03.001.03.05, 03.14.03.010.00.02 and 01.13.06.001.06.04) and Fundação de Apoio à Pesquisa do Distrito Federal (FAPDF no. 193.001.392/2016 and 193.001.197/2016). We thank FAPEMIG, CNPq and/or CAPES for providing the scholarship to TRS, CCB, MR, LPS and ESGM. The authors declare that they have no conflicts of interest.

REFERENCES

1 Considine DM and Considine GD eds, *Foods and Food Production Encyclopedia*. Springer, New York, NY (1995).
2 Sundin GW, Castiblanco LF, Yuan X, Zeng Q and Yang CH, Bacterial disease management: challenges, experience, innovation, and future prospects. *Mol Plant Pathol* **17**:1506–1518 (2016).
3 Thorley AJ and Tetley TD, New perspectives in nanomedicine. *Pharmacol Ther* **140**:176–185 (2013).
4 Bonatto CC and Silva LP, Higher temperatures speed up the growth and control the size and optoelectrical properties of silver nanoparticles greenly synthesized by cashew nutshells. *Ind Crops Prod* **58**:46–54 (2014).
5 Medda S, Hajra A, Dey U, Bose P and Mondal NK, Biosynthesis of silver nanoparticles from *Aloe vera* leaf extract and antifungal activity against *Rhizopus* sp. and *Aspergillus* sp. *Appl Nanosci* **5**:875–880 (2015).
6 Ankamwar B, Damle C, Ahmad A and Sastry M, Biosynthesis of gold and silver nanoparticles using *Emblica officinalis* fruit extract, their phase transfer and transmetallation in an organic solution. *J Nanosci Nanotechnol* **5**:1665–1671 (2005).
7 Ali M, Kim B, Belfield KD, Norman D, Brennan M and Ali GS, Inhibition of *Phytophthora parasitica* and *P. capsici* by silver nanoparticles synthesized using aqueous extract of *Artemisia absinthium*. *Phytopathology* **105**:1183–1190 (2015).
8 Rivera-Rangel RD, González-Muñoz MP, Avila-Rodriguez M, Razo-Lazcano TA and Solans C, Green synthesis of silver nanoparticles in oil-in-water microemulsion and nanoemulsion using geranium leaf aqueous extract as a reducing agent. *Colloids Surf A* **536**:60–67 (2017).
9 Silveira AP, Bonatto CC, Lopes CAP, Rivera LMR and Silva LP, Physicochemical characteristics and antibacterial effects of silver nanoparticles produced using the aqueous extract of *Ilex paraguariensis*. *Mater Chem Phys* **216**:476–484 (2018).
10 Prathna TC, Chandrasekaran N and Mukherjee A, Studies on aggregation behavior of silver nanoparticles in aqueous matrices: effect of surface functionalization and matrix composition. *Colloids Surf A* **390**:216–224 (2011).
11 Saratale RG, Saratale GD, Shin HS, Jacob JM, Pugazhendhi A, Bhaisare M *et al.*, New insights on the green synthesis of metallic nanoparticles using plant and waste biomaterials: current knowledge, their agricultural and environmental applications. *Environ Sci Pollut R* **25**:10164–10183 (2017).
12 Orzali L, Corsi B, Forni C and Riccioni L. *Chitosan in Agriculture: A New Challenge for Managing Plant Disease* (2017). Available: https://www.intechopen.com/books/biological-activities-and-application-of-marine-polysaccharides/chitosan-in-agriculture-a-new-challenge-for-managing-plant-disease [15 July 2018].
13 Chang TY, Chen CC, Cheng KM, Chin CY, Chen YH, Chen XA *et al.*, Trimethyl chitosan-capped silver nanoparticles with positive surface charge: their catalytic activity and antibacterial spectrum including multidrug-resistant strains of *Acinetobacter baumannii*. *Colloids Surf B* **155**:61–70 (2017).
14 Lin S, Chen L, Huang L, Cao S, Luo X and Liu K, Novel antimicrobial chitosan-cellulose composite films bioconjugated with silver nanoparticles. *Ind Crop Prod* **70**:395–403 (2015).
15 Matei PM, Martín-Ramos P, Sánchez-Báscones M, Hernández-Navarro S, Correa-Guimaraes A, Navas-Gracia LM *et al.*, Synthesis of chitosan oligomers/propolis/silver nanoparticles composite systems and study of their activity against *Diplodia seriata*. *Int J Polym Sci* **2015**:1–11 (2015).
16 Mansfield J, Genin S, Magori S, Citovsky V, Sriariyanum M, Ronald P *et al.*, Top 10 plant pathogenic bacteria in molecular plant pathology. *Mol Plant Pathol* **13**:614–629 (2012).
17 Liu NT, Bauchan GR, Francoeur CB, Shelton DR, Lo YM and Nou X, *Ralstonia insidiosa* serves as bridges in biofilm formation by foodborne pathogens *Listeria monocytogenes*, *Salmonella enterica*, and Enterohemorrhagic *Escherichia coli*. *Food Control* **65**:14–20 (2016).
18 Yabuuchi E, Kosako Y, Yano I, Hotta H and Nishiuchi Y, Transfer of two *Burkholderia* and an *Alcaligenes* species to *Ralstonia* gen. Nov.: proposal of *Ralstonia pickettii* (Ralston, Palleroni and Doudoroff 1973) comb. Nov., *Ralstonia solanacearum* (Smith 1896) comb. Nov. and *Ralstonia eutropha* (Davis 1969) comb. Nov. *Microbiol Immunol* **39**:897–904 (1995).
19 Elphinstone JG ed, *Bacterial Wilt Disease and the Ralstonia Solanacearum Species Complex*. American Phytopathological Society Press, St Paul, MN (2005).
20 Hayward AC ed, *Bacterial Wilt: The Disease and its Causative Agent, Pseudomonas solanacearum*. CAB International, Wallingford (1994).
21 Fegan M and Prior P, Diverse members of the *Ralstonia solanacearum* species complex cause bacterial wilts of banana. *Austral Plant Pathol* **35**:93–101 (2006).
22 Caldwell D, Kim BS and Iyer-Pascuzzi AS, *Ralstonia solanacearum* differentially colonizes roots of resistant and susceptible tomato plants. *Phytopathology* **107**:528–536 (2017).
23 Imada K, Sakai S, Kajihara H, Tanaka S and Ito S, Magnesium oxide nanoparticles induce systemic resistance in tomato against bacterial wilt disease. *Plant Pathol* **65**:551–560 (2016).
24 Wang X, Liu X and Han H, Evaluation of antibacterial effects of carbon nanomaterials against copper-resistant *Ralstonia solanacearum*. *Colloids Surf B* **103**:136–142 (2013).
25 Yang C, Zhou Y, Zheng Y, Li C, Sheng S, Wang J *et al.*, Enzymatic modification of chitosan by cinnamic acids: antibacterial activity against *Ralstonia solanacearum*. *Int J Biol Macromol* **87**:577–585 (2016).
26 Chen J, Li S, Luo J, Wang R and Ding W, Enhancement of the antibacterial activity of silver nanoparticles against phytopathogenic bacterium *Ralstonia solanacearum* by stabilization. *J Nanomater* **2016**:1–15 (2016).
27 Aravinthan A, Govarthanan M, Selvam K, Praburaman L, Selvankumar T, Balamurugan R *et al.*, Sunroot mediated synthesis and characterization of silver nanoparticles and evaluation of its antibacterial and rat splenocyte cytotoxic effects. *Int J Nanomedicine* **10**:1977–1983 (2015).
28 Rani PU, Laxmi KP, Vadlapudi V and Sreedhar B, Phytofabrication of silver nanoparticles using the mangrove associate, *Hibiscus tiliaceus* plant and its biological activity against certain insect and microbial pests. *J Biopest* **9**:167 (2016).
29 Vadlapudi V and Amanchy R, Synthesis, characterization and antibacterial activity of silver nanoparticles from red algae, *Hypnea musciformis*. *Adv Biol Res* **11**:242–249 (2017).
30 R Core Team, *R: A Language and Environment for Statistical Computing*. R Foundation for Statistical Computing, Vienna (2013).

31 Kelman A, The relationship of the pathogenicity of *Pseudomonas solanacearum* to colony appearance on a tetrazolium medium. *Phytopathology* **44**:693–695 (1934).
32 Murdock RC, Braydich-Stolle L, Schrand AM, Schlager JJ and Hussain SM, Characterization of nanomaterial dispersion in solution prior to in vitro exposure using dynamic light scattering technique. *Toxicol Sci* **101**:239–253 (2008).
33 Dennis G, Harrison W, Agnes K and Erastus G, Effect of biological control antagonists adsorbed on chitosan immobilized silica nanocomposite on *Ralstonia solanacearum* and growth of tomato seedlings. *Adv Res* **6**:1–23 (2016).
34 Kumirska J, Czerwicka M, Kaczyński Z, Bychowska A, Brzozowski K, Thöming J *et al.*, Application of spectroscopic methods for structural analysis of chitin and chitosan. *Mar Drugs* **8**:1567–1636 (2010).
35 Li P, Dai YN, Zhang JP, Wang AQ and Wei Q, Chitosan-Alginate nanoparticles as a novel drug delivery system for nifedipine. *Int J Biomed Sci* **4**:221 (2008).
36 Elbeshehy EK, Elazzazy AM and Aggelis G, Silver nanoparticles synthesis mediated by new isolates of *Bacillus* spp., nanoparticle characterization and their activity against Bean Yellow Mosaic Virus and human pathogens. *Front Microbiol* **6**:453 (2015).
37 Umadevi M, Bindhu MR and Sathe V, A novel synthesis of malic acid capped silver nanoparticles using *Solanum lycopersicums* fruit extract. *J Mater Sci Technol* **29**:317–322 (2013).
38 Kumar CG and Mamidyala SK, Extracellular synthesis of silver nanoparticles using culture supernatant of *Pseudomonas aeruginosa*. *Colloids Surf B* **84**:462–466 (2012).
39 Mittal AK, Jayeeta B, Sanjay K and Uttam CB, Biosynthesis of silver nanoparticles: elucidation of prospective mechanism and therapeutic potential. *J Colloid Interface Sci* **415**:39–47 (2014).
40 Shahverdi AR, Minaeian S, Shahverdi HR, Jamalifar H and Nohi AA, Rapid synthesis of silver nanoparticles using culture supernatants of Enterobacteria: a novel biological approach. *Process Biochem* **42**:919–923 (2007).
41 Shankar SS, Ahmad A, Pasricha R and Sastry M, Bioreduction of chloroaurate ions by geranium leaves and its endophytic fungus yields gold nanoparticles of different shapes. *J Mater Chem* **13**:1822–1826 (2003).
42 Sivaraman SK, Elango I, Kumar S and Santhanam V, A green protocol for room temperature synthesis of silver nanoparticles in seconds. *Curr Sci* **97**:1055–1059 (2009).
43 Thakkar KN, Mhatre SS and Parikh RY, Biological synthesis of metallic nanoparticles. *Nanomed Nanotechnol Biol Med* **6**:257–262 (2010).
44 Saha S, Sarkar J, Chattopadhyay D, Patra S, Chakraborty A and Acharya K, Production of silver nanoparticles by a phytopathogenic fungus *Bipolaris nodulosa* and its antimicrobial activity. *Dig J Nanomater Biostruct* **5**:887–895 (2010).
45 Jain N, Bhargava A, Majumdar S, Tarafdar JC and Panwar J, Extracellular biosynthesis and characterization of silver nanoparticles using *Aspergillus flavus* NJP08: a mechanism perspective. *Nanoscale* **3**:635–641 (2011).
46 Silva-Beltrán NP, Ruiz-Cruz S, Cira-Chávez LA, Estrada-Alvarado MI, Ornelas-Paz JDJ, López-Mata MA *et al.*, Total phenolic, flavonoid, tomatine, and tomatidine contents and antioxidant and antimicrobial activities of extracts of tomato plant. *Int J Anal Chem* **2015**:1–10 (2015).
47 Della-Pelle F, Scroccarello A, Sergi M, Mascini M, Del Carlo M and Compagnone D, Simple and rapid silver nanoparticles based antioxidant capacity assays: reactivity study for phenolic compounds. *Food Chem* **256**:342–349 (2018).
48 Sahu N, Soni D, Chandrashekhar B, Satpute DB, Saravanadevi S, Sarangi BK *et al.*, Synthesis of silver nanoparticles using flavonoids: hesperidin, naringin and diosmin, and their antibacterial effects and cytotoxicity. *Int Nano Letter* **6**:173–181 (2016).
49 Gardea-Torresdey JL, Gomez E, Peralta-Videa JR, Parsons JG, Troiani H and Jose-Yacaman M, *Alfalfa sprouts*: a natural source for the synthesis of silver nanoparticles. *Langmuir* **19**:1357–1361 (2003).
50 Krishnaraj C, Jagan EG, Rajasekar S, Selvakumar P, Kalaichelvan PT and Mohan N, Synthesis of silver nanoparticles using *Acalypha indica* leaf extracts and its antibacterial activity against water borne pathogens. *Colloids Surf B* **76**:50–56 (2010).
51 Rajathi K and Sridhar S, Room temperature synthesis of silver nanoparticles by using arial part of *Tephrosia purpurea* extract in biological method and evaluation of its antibacterial activity. *Int J Green Chem Bioprocess* **2**:39–43 (2012).
52 Thwala M, Musee N, Sikhwivhilu L and Wepener V, The oxidative toxicity of Ag and ZnO nanoparticles towards the aquatic plant *Spirodela punctuta* and the role of testing media parameters. *Environ Sci Processes Impact* **15**:1830–1843 (2013).
53 Hong J, Peralta-Videa JR, Rico C, Sahi S, Viveros MN, Bartonjo J *et al.*, Evidence of translocation and physiological impacts of foliar applied CeO_2 nanoparticles on cucumber (*Cucumis sativus*) plants. *Environ Sci Technol* **48**:4376–4385 (2014).
54 Pradas del Real AE, Vidal V, Carrière M, Castillo-Michel H, Levard C, Chaurand P *et al.*, Silver nanoparticles and wheat roots: a complex interplay. *Environ Sci Technol* **51**:5774–5782 (2017).
55 American Society for Testing and Materials (ASTM) Standard test methods for zeta potential of colloids in water and wastewater, in *The Annual Book of ASTM*, ed. by American Society for Testing and Materials Standard (ed). New York, NY, pp. 4182–4187 (1985).
56 Jannoo K, Teerapatsakul C, Punyanut A and Pasanphan W, Electron beam assisted synthesis of silver nanoparticle in chitosan stabilizer: preparation, stability and inhibition of building fungi studies. *Radiat Phys Chem* **112**:177–188 (2015).
57 Dorobantu LS, Fallone C, Noble AJ, Veinot J, Ma G, Goss GG *et al.*, Toxicity of silver nanoparticles against bacteria, yeast, and algae. *J Nanopart Res* **17**:172 (2015).
58 Radniecki TS, Stankus DP, Neigh A, Nason JA and Semprini L, Influence of liberated silver from silver nanoparticles on nitrification inhibition of *Nitrosomonas europaea*. *Chemosphere* **85**:43–49 (2011).
59 Rabea EI, Badawy MET, Stevens CV, Smagghe G and Steurbaut W, Chitosan as antimicrobial agent: applications and mode of action. *Biomacromolecules* **4**:1457–1465 (2003).
60 Wang GH, Inhibition and inactivation of five species of foodborne pathogens by chitosan. *J Food Prot* **55**:916–919 (1992).
61 Ocsoy I, Paret ML, Ocsoy MA, Kunwar S, Chen T, You M *et al.*, Nanotechnology in plant disease management: DNA-directed silver nanoparticles on graphene oxide as an antibacterial against *Xanthomonas perforans*. *ACS Nano* **7**:8972–8980 (2013).
62 Girilal M, Mohammed Fayaz A, Elumalai LK, Sathiyaseelan A, Gandhiappan J and Kalaichelvan PT, Comparative stress physiology analysis of biologically and chemically synthesized silver nanoparticles on *Solanum lycopersicum* L. *Colloid Interface Sci Commun* **24**:1–6 (2018).
63 Anjum NA, Gill SS, Duarte AC, Pereira E and Ahmad I, Silver nanoparticles in soil–plant systems. *J Nanopart Res* **15**:1896 (2013).
64 Walters DR, Ratsep J and Havis ND, Controlling crop diseases using induced resistance: challenges for the future. *J Exp Bot* **64**:1263–1280 (2013).
65 Navarro E, Baun A, Behra R, Hartmann NB, Filser J, Miao AJ *et al.*, Environmental behavior and ecotoxicity of engineered nanoparticles to algae, plants, and fungi. *Ecotoxicology* **17**:372–386 (2008).
66 Martínez-Gutierrez F, Thi EP, Silverman JM, de Oliveira CC, Svensson SL, Hoek AV *et al.*, Antibacterial activity, inflammatory response, coagulation and cytotoxicity effects of silver nanoparticles. *Nanomed Nanotechnol Biol Med* **8**:328–336 (2012).
67 Nayak BK, Chitra N and Anima N, Comparative antibiogram analysis of AgNPs synthesized from two *Alternaria* spp. with amoxicillin antibiotics. *J Chem Pharm Res* **7**:727–731 (2015).
68 Rajeshkumar S and Malarkodi C, In vitro antibacterial activity and mechanism of silver nanoparticles against foodborne pathogens. *Bioinorg Chem Appl* **2014**:581890 (2014).